JOURNAL OF SOLID STATE CHEMISTRY 118, 53–61 (1995)

Oxygen Nonstoichiometry and Crystal and Defect Structure of $PrMnO_{3+y}$ and $NdMnO_{3+y}$

V. A. Cherepanov,[1] L. Yu. Barkhatova, A. N. Petrov, and V. I. Voronin*

*Department of Chemistry, Urals A. M. Gorki State University, 51 Lenin av., Ekaterinburg 620083, Russia; and *Institute for Metal Physics, Ural Branch of RAS, 18 S. Kovalevskaya st., Ekaterinburg, GSP-170, 620219, Russia*

Received July 19, 1994; in revised form January 3, 1995; accepted January 10, 1995

Praseodymium and neodymium manganates $LnMnO_{3+y}$ have been prepared and characterized by powder X-ray and neutron diffraction together with thermogravimetric and chemical titration analysis. Both ternary oxides have an orthorhombically distorted perovskite-like structure (*Pbnm* space group) with unit cell parameters $a = 5.4562(7)$, $b = 5.5914(7)$, $c = 7.672(1)$ Å and $a = 5.4116(9)$, $b = 5.6928(9)$, $c = 7.599(1)$ Å for praseodymium and neodymium manganates, respectively. A small deficiency in manganese has been found together with an oxygen excess, which can likely be described by the cation disorder: $Pr_{0.95}Mn_{0.94}O_3$ and $Nd_{0.97}Mn_{0.95}O_3$. The thermodynamics of the oxygen exchange process have been described in terms of partial molar enthalpy and partial molar entropy of the oxygen dissolution in the lattice.

1. INTRODUCTION

Oxygen nonstoichiometry in $LnMnO_{3+y}$ has become an object of interest because of its influence on the crystal structure as well as its electrical and magnetic properties. The only rare earth manganate that has been studied in detail is $LaMnO_{3+y}$ (1–11).

It was shown that oxygen nonstoichiometry y in $LaMnO_{3+y}$ could have either positive or negative values depending on the temperature and oxygen pressure. Takeda *et al.* (9) studied the unit cell changes with oxygen nonstoichiometry in $LaMnO_{3+z}$ [$3.09 \geq (3 + z) \geq 2.99$] and suggested that oxygen excess is characterized by cation defects rather than by interstitial oxygen. Earlier Tofield and Scott (6) performed neutron studies in order to determine the nature of the ionic disorder when there was an oxygen excess in lanthanum manganate. They found that the most likely explanation of their data was cation vacancies described by the formula as: $(La_{0.94\pm0.02}[\ ]_{0.06\pm0.02})(Mn^{3+}_{0.745}Mn^{4+}_{0.235}[\ ]_{0.02})O_3$. The authors discussed different ways of incorporating lanthanum surplus (in comparison with manganese) losses, but there was no evidence of La_2O_3 as a second phase. The ability of lanthanum manganate to form the A-site deficiency, such as $La_{1-y}MnO_{3+z}$, where y reached values up to 0.1 was confirmed later (9, 10). Similar rare earth deficiency for praseodymium manganate $Pr_{1-x}Mn_{1+x}O_3$ had been found by Pollert and Jirak (12); however, they explained it in terms of the partial substitution of Mn for Pr.

Negative values of y had been obtained at relatively low oxygen partial pressure (7, 11).

The oxygen nonstoichiometry in $NdMnO_{3+x}$ as a function of oxygen pressure was studied by Kamegashira and Miyazaki (13) at 1273 K. The maximum deviation from stoichiometric oxygen content was found to be 0.065 when heated to 1273 K under oxygen ($P_{O_2} = 1$ atm). There appears to be no more information about oxygen nonstoichiometry in praseodymium and neodymium manganates in the literature.

2. EXPERIMENTAL

Praseodymium oxide (Pr_6O_{11}), neodymium oxide (Nd_2O_3), and manganese oxide (Mn_2O_3) with purities >99.9% were used as starting materials. Before preparation of the samples all starting materials were annealed in air: Pr_6O_{11} at 480°C; Nd_2O_3 at 1200°C, and Mn_2O_3 at 700°C.

The samples of $PrMnO_{3+y}$ and $NdMnO_{3+y}$ were prepared by the usual ceramic technique of three-stage firing in air in the temperature range 850–1200°C for 15–20 hr at each stage with intermediate regrinding in an agate mortal. The synthesis of the ternary oxides can be represented by the equations:

$$Pr_6O_{11} + 3Mn_2O_3 = 6PrMnO_{3+y} + (1 - 3y)O_2 \quad [1]$$

$$Nd_2O_3 + Mn_2O_3 + yO_2 = 2NdMnO_{3+y}. \quad [2]$$

Both samples were identified by X-ray powder diffraction as single phase.

For the structural investigations and chemical analysis the samples of single phase $LnMnO_{3+y}$ were first annealed

[1] To whom correspondence should be addressed.

0022-4596/95 $12.00

in air at 1173 K for 24 hr, slowly cooled to 973 K, fired at this temperature for 70 hr, and allowed to cool in the furnace to room temperature.

The crystal structures of both $PrMnO_{3+y}$ and $NdMnO_{3+y}$ were refined from X-ray and neutron diffraction measurements. XRD patterns were obtained using the UM-1 diffractometer with copper radiation. Powder neutron profiles of $LnMnO_{3+y}$ were measured at the IVV-2 research reactor located near Ekaterinburg, Russia, on the D7A diffractometer with a double monochromator (002) reflection of a single crystal of pyrolytic graphite and (333) reflection of germanium. The wavelength employed was 1.515 Å. The collected data were refined by the Rietveld profile method using the FULLPROF program (14).

The changes in oxygen nonstoichiometry were determined using the TGA technique in the temperature range 1120–1480 K at an oxygen pressure of $1 - 6 \times 10^{-4}$ atm. Different oxygen pressures were obtained by mixing helium or nitrogen with air or oxygen in the appropriate ratios and measured using an oxygen sensor (ZrO_2 doped with Y_2O_3) which was located just under the sample in the TGA cell. The control of the thermodynamic parameters was accurate to $\Delta \log(P_{O_2}/\text{atm}) = \pm 0.05$; $\Delta T = \pm 0.5$ K; the maximum error in measuring weight changes was $\pm 2 \times 10^{-3}\%$.

The thermodynamic equilibrium weights were confirmed by reproducing them from lower and higher temperatures, by varying oxygen pressure, or by using different samples. The period required to establish equilibria between the gaseous phase and the sample varied from 3 to 24 hr, depending on the temperature and oxygen partial pressure range involved.

The absolute value of y was determined by the direct reduction of the sample in the TGA cell by a hydrogen flux, according to the reaction

$$2LnMnO_{3+y} + [3 + 2y - 2/(1 - \gamma)]H_2 = Ln_2O_3 + 2/(1 - \gamma)Mn_{1-\gamma}O + [3 + 2y - 2/(1 - \gamma)]H_2O. \quad [3]$$

X-ray diffraction patterns confirmed that praseodymium (III) (or neodymium (III)) oxide Ln_2O_3 and manganese (II) oxide $Mn_{1-\gamma}O$ were the only phases found after reduction.

Chemical determination of the oxidation state of the manganese ions was performed by chromatometric titration. The samples were dissolved in a hot solution of HCl with a predetermined excess of $FeCl_2$ under a layer of paraffin (in order to prevent the oxidation of Fe^{2+} in air). The reaction which took place during this process can be written as $Mn^{4+} + Fe^{2+} = Mn^{3+} + Fe^{3+}$. The concentration of Mn^{4+} was deduced from the number of Fe^{2+} ions that remained by titration with $K_2Cr_2O_7$ solution.

3. RESULTS AND DISCUSSION

3.1. Crystal Structure

Inspection of the X-ray and neutron diffraction profiles (Figs. 1 and 2) shows that both praseodymium and neodymium manganates are satisfactorily described by the *Pbnm* (No. 62) space group (orthorhombically distorted perovskite-like structure). Final structural parameters derived from the Rietveld profile refinement of X-ray and neutron diffraction measurements are listed in Table 1. The results obtained indicate that oxygen excess in $LnMnO_{3+y}$ can be satisfactorily described by vacancies in the cation sublattices. Based on the structural parameters, interatomic distances were calculated (Table 2). The structure of the manganates can be represented by a lattice built up from distorted MnO_6 octahedra joined by apexes. The Mn–O interatomic distances in these octahedra are

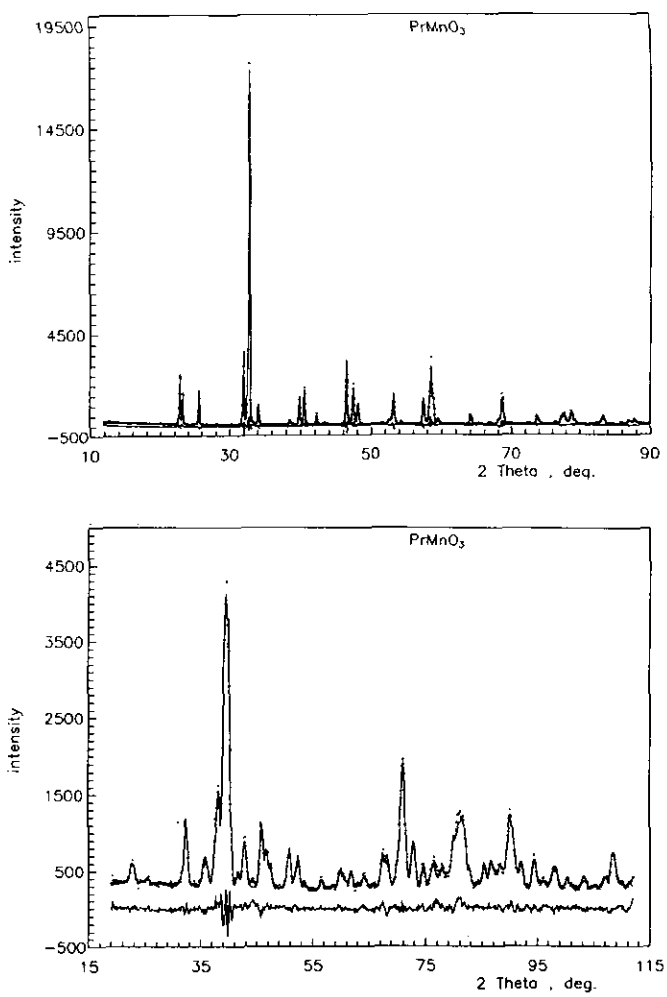

FIG. 1. Observed (points) and calculated (line) X-ray (top) and neutron diffraction (bottom) profiles for $PrMnO_{3+y}$. The difference profiles are also shown.

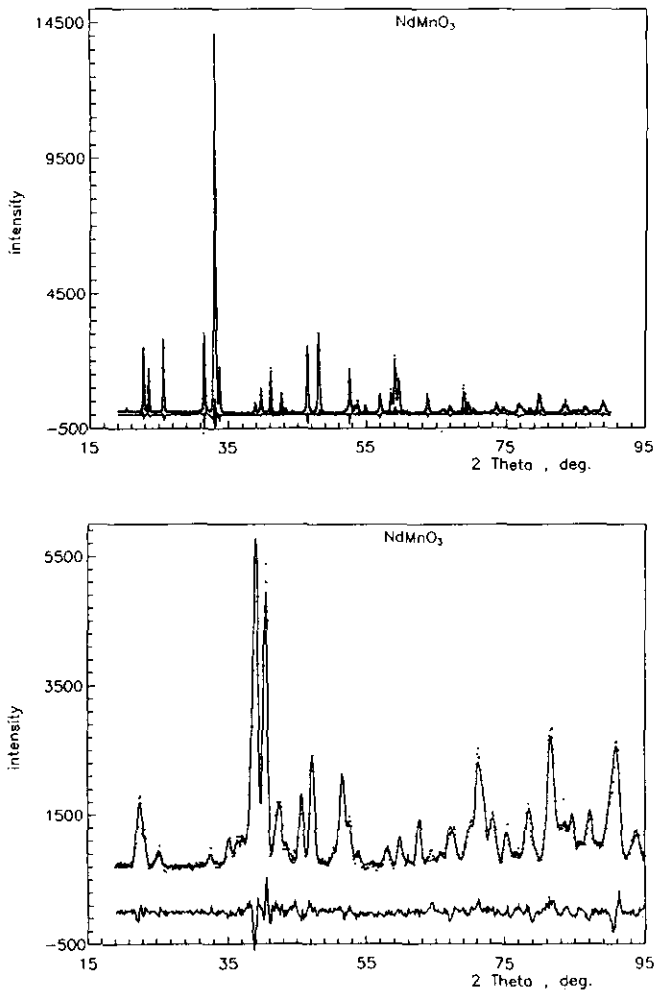

FIG. 2. Observed (points) and calculated (line) X-ray (top) and neutron diffraction (bottom) profiles for $NdMnO_{3+y}$. The difference profiles are also shown.

1.966, 1.945, and 2.062 Å in $PrMnO_{3+y}$ and 1.956, 1.953, and 2.099 Å in $NdMnO_{3+y}$.

3.2. Oxygen Nonstoichiometry

Calculation from TGA measurements of the oxygen nonstoichiometry at different temperatures and oxygen pressures requires the determination of a starting point. This was determined after TGA measurements in the range of homogeneity of $LnMnO_{3+y}$, which had been reported previously (15), by direct reduction of the sample by H_2 (reaction 3).

It is known that the oxygen nonstoichiometry of rare earth oxides is negligible (16). The composition of $Mn_{1-y}O$ has been studied as a function of T and P_{O_2} (17) in detail. It changes from stoichiometric MnO to $MnO_{0.993}$ in the oxygen activity range 10^{-16}–10^{-20} atm at 1173 K. The reduction by hydrogen and calculation of absolute values of oxygen nonstoichiometry y were made on the samples that had first been equilibrated at 1173 K, $P_{O_2} = 0.21$ atm. Each ternary oxide was reduced at least three times. The results obtained were reproducible within the accuracy of the method: y(1173 K, air) = 0.072 ± 0.003 for $PrMnO_{3+y}$ and y(1173 K, air) = 0.058 ± 0.006 for $NdMnO_{3+y}$.

The reversibility of mass changes during TGA experiments proves that there were no other exchanges between solid and gaseous phases except those involving oxygen. Using the absolute values of y at 1173 K in air and the results of the mass change measurements, the absolute values of y at all T and P_{O_2} were calculated. The calculation scheme used was described in (18). The oxygen content in $LnMnO_{3+y}$ as a function of temperature at different oxygen pressures is shown in Fig. 3. The dependency of log y vs $(1/T)$ (Fig. 4) is satisfactorily described by linear equations whose coefficients are listed in Table 3. Isothermal cross sections of temperature dependences give us the plots of oxygen nonstoichiometry vs oxygen partial pressure (Fig. 5).

3.3. Defect Structure

The process of cation disorder of the ideal $LnMnO_3$ crystal structure which leads to the oxygen excess can be written as

$$3/2O_2 = 3O_O^x + V_{Ln}''' + V_{Mn}''' + 6h^{\cdot}. \qquad [4]$$

Here and later in this paper Kröger–Vink notation (19) is used.

The holes captured by manganese ions transform Mn^{3+} to Mn^{4+}. It may be better to say that the tendency of Mn^{3+} to increase partially its oxidation state under particular conditions and in particular surroundings is a driving force for the appearance of oxygen excess. We will return to this point later.

Recent data reported by van Roosmalen and Huijsmans (10) show that there is a partial charge disproportionation of Mn^{3+} into Mn^{4+} and Mn^{2+} at high temperature

$$2Mn^{3+} = Mn^{2+} + Mn^{4+}, \qquad [5]$$

which may also be represented by

$$\text{nil} = e' + h^{\cdot}. \qquad [6]$$

This should be taken into consideration together with process [4]. If we assume that at relatively low oxygen pressure (but higher than the decomposition pressure) oxygen deficiency can be represented by oxygen vacancies and process [4] takes place at higher oxygen pressure, the diagram of defect equilibria and hence oxygen nonstoichiometry as a function of P_{O_2} could be constructed (Fig.

TABLE 1
Final Structural Parameters of $PrMnO_{3+y}$ and $NdMnO_{3+y}$

	X	S_X	Y	S_Y	Z	S_Z	B	S_B	OCC	S_{OCC}
					$PrMnO_{3+y}$ neutron diffraction					
Mn	0.5000	0.0000	0.0000	0.0000	0.0000	0.0000	0.37	0.07	0.939	0.013
Pr	−0.0069	0.0013	0.0451	0.0009	0.2500	0.0000	0.65	0.07	0.950	0.010
O1	0.0770	0.0007	0.4825	0.0007	0.2500	0.0000	0.63	0.09	1.000	0.000
O2	−0.2844	0.0005	0.2978	0.0005	0.0404	0.0004	0.76	0.08	2.000	0.000
Cell parameters: 5.4562(7), 5.5914(7), 7.672(1)										
Overall temp. factor = 0.0000, 0.0000										
*R*p + 5.52 *R*wp = 7.11 *R*exp = 4.27 CHI2 = 2.771										
Derived Bragg R-factor 5.94										
*R*f-factor 4.10										
					$PrMnO_{3+y}$ X-ray diffraction					
Mn	0.5000	0.0000	0.0000	0.0000	0.0000	0.0000	0.50	0.00	0.982	0.017
Pr	−0.0088	0.0005	0.0458	0.0003	0.2500	0.0000	0.50	0.00	0.960	0.017
O1	0.0766	0.0034	0.4847	0.0027	0.2500	0.0000	0.50	0.00	1.000	0.000
O2	−0.2831	0.0029	0.2921	0.0024	0.0381	0.0017	0.50	0.00	2.000	0.000
Cell parameters: 5.4559(2), 5.5941(2), 7.6635(3)										
*R*p = 9.53 *R*wp = 12.98 *R*exp = 5.92 CHI2 = 4.811 L. S. refinement										
Conventional Rietveld *R*p, *R*wp, *R*e, and CHI2: 13.81 16.59 7.56 4.811										
Derived Bragg factor 5.75										
*R*f-factor 6.40										
					$NdMnO_{3+y}$ neutron diffraction					
Mn	0.5000	0.0000	0.0000	0.0000	0.0000	0.0000	0.50	0.00	0.950	0.017
Nd	−0.0135	0.0010	0.0595	0.0009	0.2500	0.0000	0.50	0.00	0.973	0.010
O1	0.0833	0.0010	0.4803	0.0010	0.2500	0.0000	0.50	0.00	1.000	0.000
O2	−0.2912	0.0008	0.3054	0.0008	0.0426	0.0005	0.50	0.00	2.000	0.000
Cell parameters: 5.4116(9), 5.6928(9), 7.599(1)										
Overall temp. factor = −0.0624, 0.0620										
*R*p = 4.89 *R*wp = 6.23 *R*exp = 2.86 CHI2 = 4.749										
Derived Bragg R-factor 7.15										
*R*f-factor 5.30										
					$NdMnO_{3+y}$ X-ray diffraction					
Mn	0.5000	0.0000	0.0000	0.0000	0.0000	0.0000	0.50	0.00	0.960	0.018
Nd	−0.0123	0.0005	0.0603	0.0003	0.2500	0.0000	0.50	0.00	0.965	0.018
O1	0.0953	0.0031	0.4737	0.0029	0.2500	0.0000	0.50	0.00	1.000	0.000
O2	−0.2798	0.0029	0.2986	0.0025	0.0431	0.0019	0.50	0.00	2.000	0.000
Cell parameters: 5.4059(2), 5.6925(2), 7.5877(3)										
Overall temp. factor = 0.0000, 0.0000										
*R*p = 9.12 *R*wp = 12.27 *R*exp = 5.89 CHI2 = 4.333 L. S. refinement										
Conventional Rietveld Rp, Rwp, Re and CHI2: 12.26 15.21 7.31 4.333										
Derived Bragg R-factor 5.14										
*R*f-factor 4.35										

6) using the Broüwer approximation method (19). Thus one can expect that y will approach zero as oxygen pressure decreases; but according to the experimental results, it tends toward some constant value which is close, but not equal to zero. The most probable reason for such a discrepancy could be a deviation of the Ln : Mn ratio from 1 : 1. The absolute values of the oxygen nonstoichiometry y used as a starting point were calculated according to the reaction [3] for Ln : Mn = 1 : 1. However, the results of structural refinement gave the probabilities of metal atom occupation, which have led to the following formulas: $Pr_{0.95}Mn_{0.94}O_3$ and $Nd_{0.97}Mn_{0.95}O_3$. This shows that together with oxygen excess, rare earth manganates can possess metal deficiency either in rare earth metal (6, 9, 12) or in manganese, as in our case. The appearance of manganese deficiency is probably caused by the ability of manganese oxide to react with the alumina crucibles during synthesis, which leads to the formation of additional manganese vacancies:

$$\tfrac{3}{4}O_2 \xrightarrow[-1/2Mn_2O_3]{} V'''_{Mn} + 3h^{\cdot} \qquad [7]$$

TABLE 2
Interatomic Distances in $PrMnO_{3+y}$ and $NdMnO_{3+y}$

	Coordination number	$PrMnO_{3+y}$	$NdMnO_{3+y}$
Mn–Mn	2	3.8360(3)	3.7994(5)
	4	3.9062(4)	3.9272(6)
Mn–*Ln*	2	3.186(4)	3.147(4)
	2	3.314(6)	3.264(4)
	2	3.375(6)	3.383(5)
	2	3.601(4)	3.709(4)
Mn–O1	2	1.9659(9)	1.956(1)
Mn–O2	2	1.945(3)	1.953(4)
	2	2.062(3)	2.099(4)
Ln–*Ln*	2	3.854(9)	3.828(7)
	2	3.870(1)	3.862(1)
	2	3.959(9)	4.029(7)
Ln–O1	1	2.372(8)	2.371(8)
	1	2.488(6)	2.452(8)
	1	3.130(8)	3.116(8)
	1	3.179(6)	3.339(8)
Ln–O2	2	2.407(5)	2.386(6)
	2	2.622(6)	2.589(6)
	2	2.685(5)	2.642(5)
	2	3.342(5)	3.461(6)

The absolute values of oxygen nonstoichiometry were recalculated taking into account manganese deficiency according to the reactions:

$$Pr_{0.95}Mn_{0.94}O_3 + (0.635 - 1.575\gamma)/(1 - \gamma)H_2 = 4.475Pr_2O_3 + 0.94/(1 - \gamma)Mn_{1-\gamma}O + (0.635 - 1.575\gamma)/(1 - \gamma)H_2O \quad [8]$$

$$Nd_{0.97}Mn_{0.95}O_3 + (0.595 - 1.545\gamma)/(1 - \gamma)H_2 = 0.485Nd_2O_3 + 0.95/(1 - \gamma)Mn_{1-\gamma}O + (0.595 - 1.545\gamma)/(1 - \gamma)H_2O. \quad [9]$$

This gave lower values of y(1173 K, air), which brought the observed results closer to the theoretical values. However, recalculation of all dependences have not been made because different samples synthesized independently were used for the TGA and structural measurements. The concentration of so-called "biographical" defects, i.e., manganese deficiency, could be different in each sample.

Although the deficiency in one of the metal components is not directly accompanied by changes in oxygen content (reaction [7], or a similar reaction with a rare earth oxide), it leads to an increase in the hole concentration, i.e., the average oxidation state of the manganese ions, which influence the defect equilibria as a whole. The results of Takeda *et al.* (9) show that an increase in the lanthanum deficiency (Y) in $La_{1-Y}MnO_{3+Z}$ leads to a decrease in the oxygen excess (Z) at a practically constant oxidation state of manganese. In that case manganese ions partially increased their oxidation state from +3 (to achieve a Mn^{3+}/Mn^{4+} ratio which corresponds to the equilibrium oxidation potential for the experimental conditions) due to rare earth deficiency together with oxygen excess. So, the thermodynamically advantageous average oxidation state of 3*d*-transition metal determined equilibria of the defects, i.e., nonstoichiometry (oxygen or metal), which could vary in correlation to each other in order to keep Mn^{3+}/Mn^{4+} ratio approximately constant. Maximum oxygen excess can be obtained in the sample with the Ln : Mn ratio equal to 1 : 1.

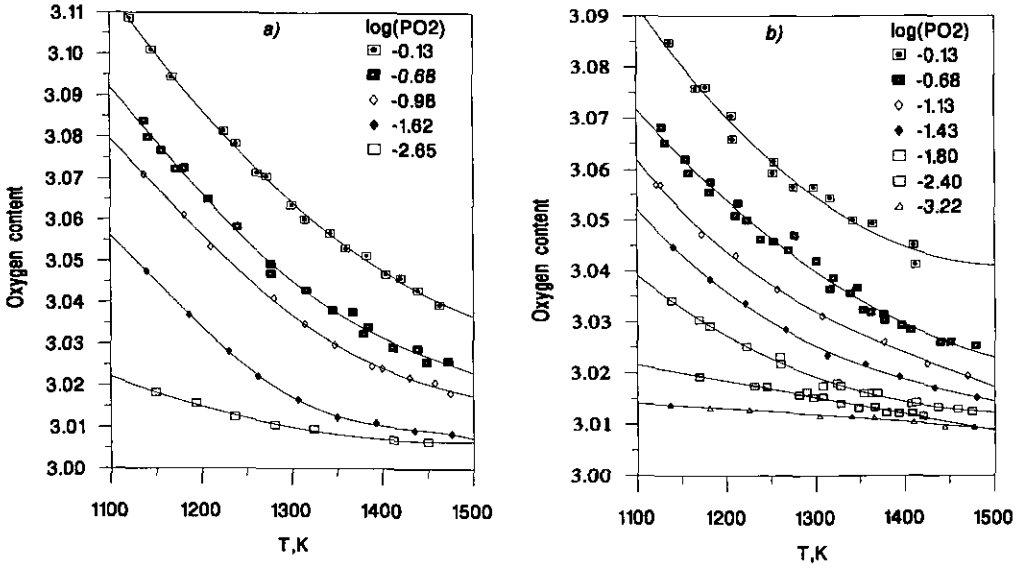

FIG. 3. Oxygen content in $PrMnO_{3+y}$ (a) and $NdMnO_{3+y}$ (b) *vs temperature at different oxygen pressures* P_{O_2}.

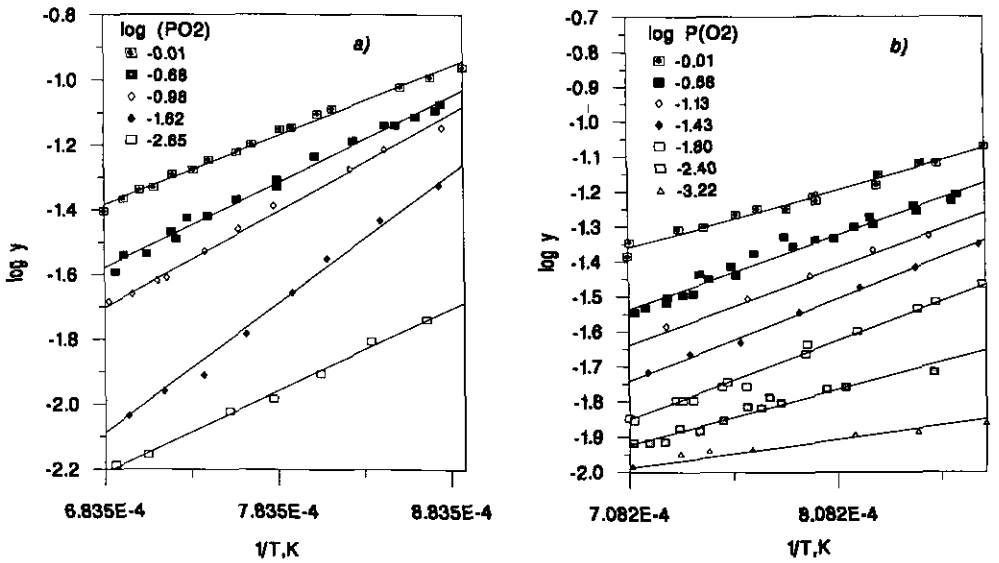

FIG. 4. The logarithm of oxygen nonstoichiometry in $PrMnO_{3+y}$ (a) and $NdMnO_{3+y}$ (b) vs inverse temperature at different oxygen pressures.

Let us assume that the starting stoichiometric (with respect to oxygen) composition is $Ln\mathrm{Mn}^{3+}_{1-4n}\mathrm{Mn}^{4+}_{3n}\mathrm{O}_3$, where n is the manganese deficiency in the sample due to its prehistory. Then the composition of the disordered oxide due to the oxygen exchange process can be written as $Ln_{1-k}\mathrm{Mn}^{3+}_{1-4n-7k}\mathrm{Mn}^{4+}_{3n+6k}\mathrm{O}_3$.

Chemical analysis of $NdMnO_{3+y}$ gave the Mn^{4+} fraction $[Mn^{4+}]/([Mn^{3+}] + [Mn^{4+}]) = 0.277$. If, in the chemical formula written above for the disordered manganate, we take $k = 0.03$ according to the neutron diffraction refinement, a value of the initial manganese deficiency n can be calculated. It has been found to be $n = 0.027$. This value is in good agreement with $n = 0.023$, according to the neutron diffraction refinement, especially in light of the fact that both samples were synthesized independently. Such good agreement can arise if the homogeneity range of the manganese deficiency is narrow and the limiting composition has been achieved in all cases. However, this statement needs to be proved by experiments.

The calculation of the Mn^{4+} fraction, based on the formulas obtained from the neutron diffraction studies of $Pr_{0.95}Mn_{0.94}O_3$ and $Nd_{0.97}Mn_{0.95}O_3$, the electroneutrality condition, and the assumption that oxygen and rare earth ions have unchangeable oxidation states O^{2-} and Ln^{3+},

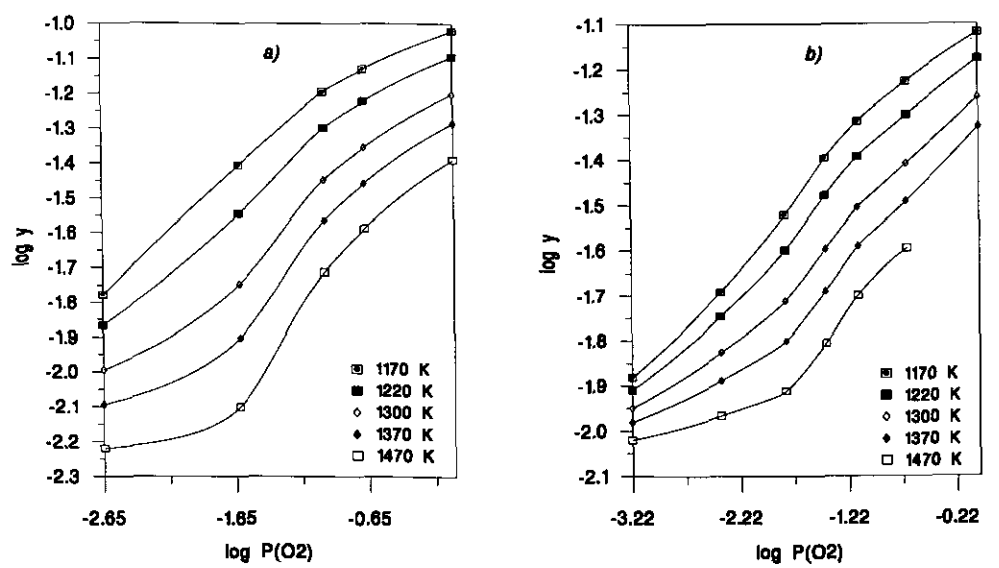

FIG. 5. The logarithm of oxygen nonstoichiometry in $PrMnO_{3+y}$ (a) and $NdMnO_{3+y}$ (a) and $NdMnO_{3+y}$ (b) vs oxygen partial pressure at different temperatures.

TABLE 3
Coefficients of Isobaric Dependences of Oxygen Nonstoichiometry in $PrMnO_{3+y}$ and $NdMnO_{3+y}$

$PrMnO_{3+y}$			$NdMnO_{3+y}$		
$\log P_{O_2}$	$-a$	$b \times 10^{-3}$	$\log P_{O_2}$	$-a$	$b \times 10^{-3}$
−0.01	2.823	2.109	−0.01	2.533	1.654
−0.68	3.369	2.618	−0.68	3.037	2.118
−0.98	3.733	2.970	−1.13	3.202	2.207
−1.62	4.807	3.978	−1.43	3.408	2.353
−2.65	3.942	2.532	−1.80	3.440	2.245
			−2.40	3.038	1.575
			−3.22	2.559	0.792

Note. $\log y = a + b \cdot T^{-1}$.

allows one to rewrite these formulas as

$$Pr_{0.95}Mn^{3+}_{0.61}Mn^{4+}_{0.33}O_3 \quad \text{and} \quad Nd_{0.97}Mn^{3+}_{0.71}Mn^{4+}_{0.24}O_3. \quad [10]$$

According to the concept of the determination of the valence–bond parameters (20), it is possible to estimate the probability of the site occupation by the manganese ions in the different oxidation states. Using the interatomic distances (Table 2), the probabilities of the site occupation by Mn^{3+} and Mn^{4+} were calculated. This gives the following formulas of the ternary oxides

$$Pr_{0.95}Mn^{3+}_{0.72}Mn^{4+}_{0.22}O_3 \quad \text{and} \quad Nd_{0.97}Mn^{3+}_{0.80}Mn^{4+}_{0.15}O_3. \quad [11]$$

The lower values of the Mn^{4+} fraction can be explained from the point of view of the partial covalency of the bonding in the manganates. The model of absolute ionic bonding, i.e., using the formal oxidation states, is true when the process of the total disintegration of the structure (in the process of reduction under H_2 or during dissolution in an acid medium before the chemical analysis) takes place. However, it is known that the effective charge of the ions in the lattice is usually lower than their formal charge, because the distribution of the valence electron density cannot be described by an ionic bonding model alone. In terms of the defect structure, the results represented in formulas [11] indicate that the effective charges of the cation vacancies are lower than their formal charges. These effective charges can be estimated using the equation of electroneutrality

$$m_1[V^{m_1'}_{Ln}] + m_2[V^{m_2'}_{Mn}] = p, \quad [12]$$

where m_1 and m_2 are the effective charge of the rare earth and manganese vacancies, respectively. If in the first approximation we assume that $m_1 \approx m_2 \approx m$, then Eq. [12] can be transformed to

$$m\{[V^{m'}_{Ln}] + [V^{m'}_{Mn}]\} = p. \quad [13]$$

The average effective charge of the cation vacancies m obtained from Eq. [13] and formulas [11] are $m \approx 2.0$ for praseodymium manganate and $m \approx 1.9$ for neodymium manganate.

3.4. *Thermodynamics of the Oxygen Exchange Process*

The thermodynamics of the oxygen exchange processes are often described in terms of the molar Gibbs potential of oxygen dissolution in the crystal structure

$$\begin{aligned}\Delta\overline{G}^{O}(O_2) &= 2.303{*}R{*}T{*}\log P_{O_2} \\ &= \Delta\overline{H}^{O}(O_2) - T{*}\Delta\overline{S}^{O}(O_2),\end{aligned} \quad [14]$$

where $\Delta\overline{G}^{O}(O_2)$, $\Delta\overline{H}^{O}(O_2)$, and $\Delta\overline{S}^{O}(O_2)$ are the partial molar Gibbs potential, partial molar enthalpy, and partial molar entropy of the oxygen-dissolving process, respectively. According to Eq. [14], the partial molar enthalpy $\Delta\overline{H}^{O}(O_2)$ and partial molar entropy $\Delta\overline{S}^{O}(O_2)$ can be obtained as

$$\Delta\overline{H}^{O}(O_2) = 2.303{*}R{*}[d\log P_{O_2}/d(1/T)]_y \quad [15]$$

$$\Delta\overline{S}^{O}(O_2) = -2.303{*}R{*}[d(T{*}\log P_{O_2})/dT]_y, \quad [16]$$

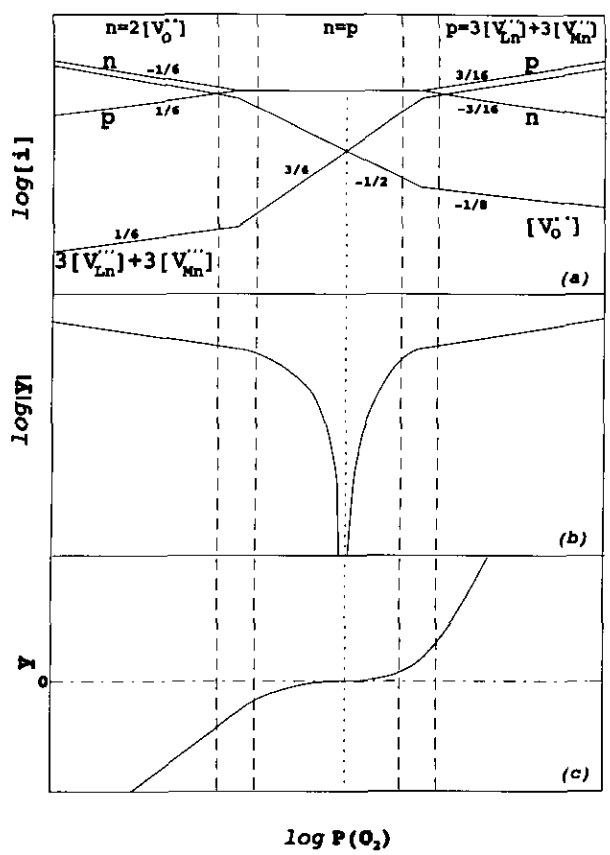

FIG. 6. Broüwer diagram of equilibrium concentration of defects (a) and oxygen nonstoichiometry (b,c) vs oxygen partial pressure.

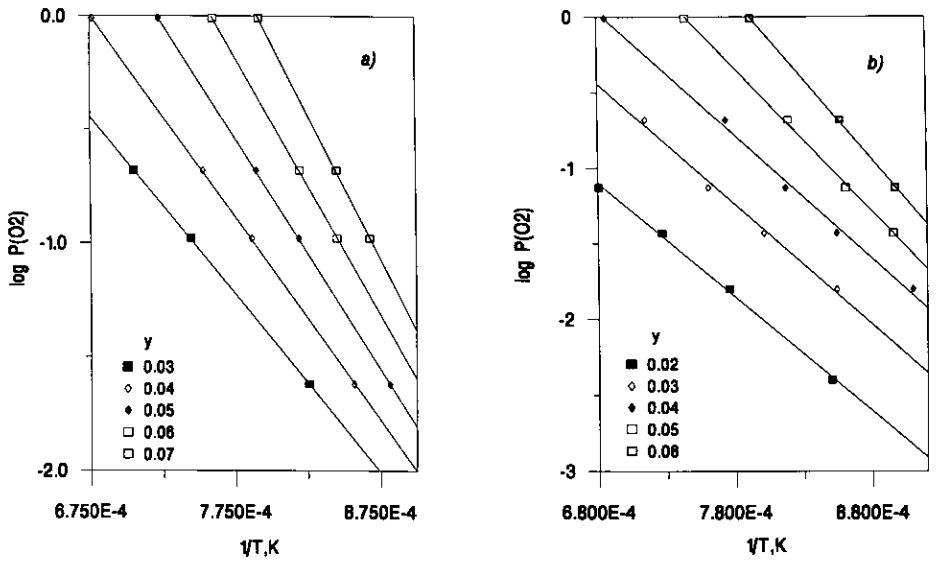

FIG. 7. Equilibrium oxygen pressure vs inverse temperature at a fixed oxygen content in $PrMnO_{3+y}$ (a) and $NdMnO_{3+y}$ (b).

i.e., the slopes of the plots of log P_{O_2} vs $1/T$ and T*log P_{O_2} vs T at constant y give the partial molar enthalpy $\Delta\overline{H}^{O}(O_2)$ and partial molar entropy $\Delta\overline{S}^{O}(O_2)$. The values of equilibrium oxygen pressures and corresponding temperatures (or inverse temperatures) at constant y were obtained using the data in Table 3. Both log P_{O_2} vs $1/T$ and T*log P_{O_2} vs T can be described as linear (Figs. 7 and 8). Therefore, $\Delta\overline{H}^{O}(O_2)$ and $\Delta\overline{S}^{O}(O_2)$ are considered to be constant at a fixed composition of complex oxide. The concentration dependences of $\Delta\overline{H}^{O}(O_2)$ and $\Delta\overline{S}^{O}(O_2)$ (Fig. 9) are very close for praseodymium and neodymium manganates. The proximity of the $\Delta\overline{S}^{O}(O_2)$ dependences can be explained by the predominant contribution of the ΔS_{conf} term for the process of oxygen dissolution. The closeness of $\Delta\overline{H}^{O}(O_2)$ shows that the difference in rare earth elements does not strongly affect the energy of the oxygen exchange process, which is mainly determined by the oxidation state of the manganese ions.

4. CONCLUSION

The crystal structure of praseodymium and neodymium manganates have been studied by X-ray and neutron diffraction methods. Both oxides have orthorhombic (*Pbnm*, (No. 62) space group) structure and the oxygen excess is accompanied by a small manganese deficiency. The re-

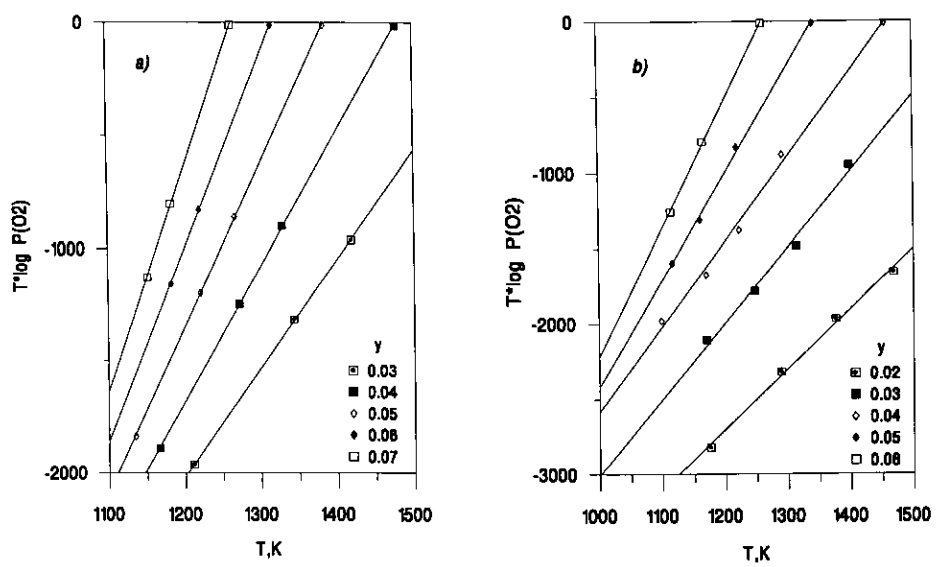

FIG. 8. Equilibrium oxygen pressure multiplied by temperature vs temperature at fixed oxygen content in $PrMnO_{3+y}$ (a) and $NdMnO_{3+y}$ (b).

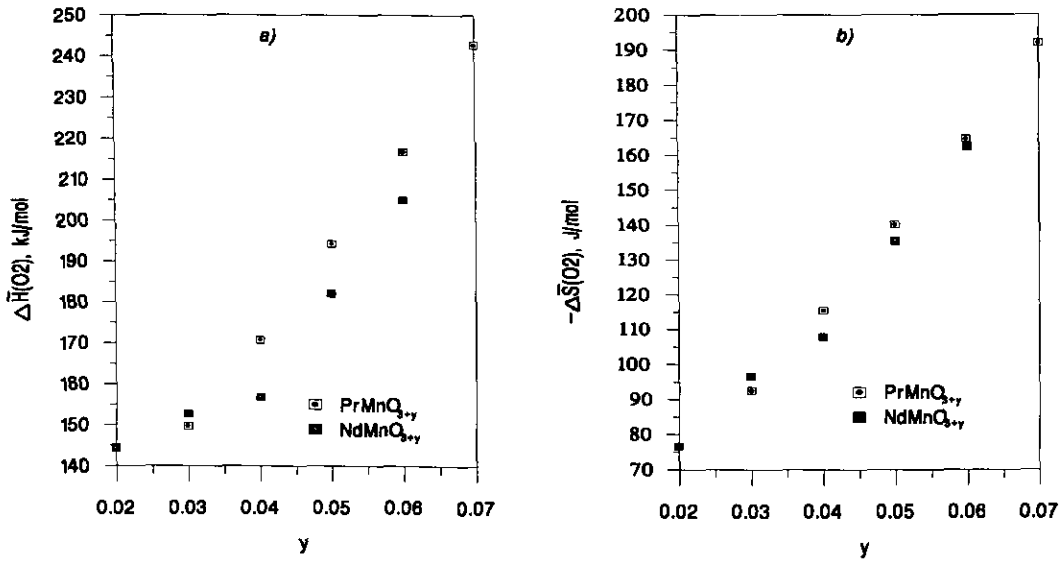

FIG. 9. Partial molar enthalpy (a) and partial molar entropy (b) of the process of oxygen dissolution vs oxygen nonstoichiometry.

sults obtained by neutron diffraction and TGA methods were confirmed by chromatometric titration. The thermodynamics of the oxygen exchange process have been described in terms of the partial molar enthalpy and the partial molar entropy of oxygen dissolution in the lattice.

ACKNOWLEDGMENTS

This work was partly supported by Grant RGJ000 from the International Science Foundation and by Grant 94-03-08153 from the Russian Fundamental Science Foundation.

REFERENCES

1. K. Kamata, K. Nakajima, T. Hayashi, and T. Nakamura, *Mater. Res. Bull.* **13,** 49 (1978).
2. G. Matsumoto, *J. Phys. Soc. Jpn.* **29,** 606 (1970).
3. T. Nakamura, G. Petzow, and L. G. Gaukler, *Mater. Res. Bull.* **14,** 649 (1979).
4. A. K. Bogush, V. I. Pavlov, and L. V. Balyko, *Cryst. Res. Technol.* **18,** 589 (1983).
5. V. I. Pavlov, A. K. Bogush, and L. V. Balyko, *Cryst. Res. Technol.* **19,** 237 (1984).
6. B. C. Tofield and W. C. Scott, *J. Solid State Chem.* **10,** 183 (1974).
7. F. Abbattista and M. L. Borlera, *Ceram. Int.* **7,** 137 (1981).
8. J. H. Kuo, H. U. Anderson, and D. M. Sparlin, *J. Solid State Chem.* **83,** 52 (1989).
9. Y. Takeda *et al. Mater. Res. Bull.* **26,** 153 (1991).
10. J. A. M. van Roosmalen, J. P. P. Huijsmans, and L. Plomp, *Solid State Ionics* **66,** 279 (1993).
11. J. A. M. van Roosmalen and E. H. P. Cordfunke, *J. Solid State Chem.* **93,** 212 (1991).
12. E. Pollert and Z. Jirak, *J. Solid State Chem.* **35,** 262 (1980).
13. N. Kamegashira and I. Miyazaki, *Mater. Res. Bull.* **19,** 1201 (1984).
14. J. Rodrigues-Carvaial, in "Abstracts Satel. Meet. Powd. Diffr., XV Congr. Int. Union Cryst., Toulose, 1990." p. 127.
15. V. A. Cherepanov, L. Yu. Barkhatova, and A. N. Petrov, *J. Phys. Chem. Solids* **55,** 229 (1994).
16. P. Kofstad, "Nonstoichiometry, Diffusion and Electrical Conductivity in Binary Oxides," p. 213, Wiley-Interscience, New York, 1972.
17. I. Arabski and C. Carel, *Bull. Soc. Bretagne* **55,** 125 (1983).
18. A. N. Petrov, V. A. Cherepanov, O. F. Kononchyk, and L. Yu. Gavrilova, *J. Solid State Chem.* **87,** 69 (1990).
19. F. A. Kröger, "The Chemistry of Imperfect Crystals." North-Holland, Amsterdam 1964.
20. I. D. Brown and D. Altermatt, *Acta Crystallogr. Sect. B* **41,** 244 (1985).